Revisiting Rectennas For Low-Power RF Power Transmission: Non-Linear Antenna-Circuit Co-Design and Multi-Diversity Antennas

Mahmoud Wagih

James Watt School of Engineering, University of Glasgow, G12 8QQ
School of Electronics and Computer Science, University of Southampton, SO17 1BJ

Abstract

This paper details multiple approaches for designing high-efficiency and high-sensitivity rectennas for low-power internet of things applications. First, impedance matching and tuning methods used to minimize diode losses are summarized. The ability to rectify µW inputs at sub-1 GHz frequencies with an RF-to-DC efficiency in excess of 40% at −20 dBm using commercial Schottky diodes is demonstrated based on antenna-circuit co-design and matching network elimination. Two demonstrators integrating the antenna-rectifier co-design approach are presented. The first is a novel shared-area simultaneous wireless information and power transfer (SWIPT) antenna, evolved from a standard microstrip patch. The SWIPT antenna achieves state-of-the-art performance, both as a communication antenna and a rectenna, while being implemented using flexible materials for wearable applications. The second example aims to scale up the DC power output from µW/cm^2 power densities, based on an array of tightly-coupled electrically-small co-designed rectennas. The thin and flexible array shows, for the first time, an effective area exceeding its physical aperture, and its DC output is compared to several prior works showing a higher efficiency. The challenge of transitioning low-cost rectennas realized on low-cost flexible substrates (e.g. organic polymers and textiles) to mmWave bands using hybrid RFIC packaging is finally reviewed. Using a GaAs diode bonded onto a textile-based microstrip matching network and broadband antenna, the first rectenna capable of harvesting mmWave power in the 5G 26/28 GHz bands is shown.

1 Introduction

Emerging in the 1950s for powering Unmanned Autonomous Vehicles (UAVs), RECTifying anteNNA (rectennas) have gone to attract significant interest for various applications [1], including microwave solar power beaming [2] and RFID [3]. The decline in the power consumption of computing, sensing, and communication systems has motivated a re-adaptation of rectennas for recycling ambient RF power, i.e. RF energy harvesting [4], or for long-range wireless power transfer (WPT) and simultaneous wireless information and power transfer (SWIPT) to sensor nodes [5]. Nevertheless, harvesting and rectifying very low RF power levels, as well as scaling low-cost rectennas based on commercial Schottky diodes to mmWave frequency bands continue to hinder the wide-scale adoption of RF WPT.

In this paper, the key challenges in rectenna-based WPT are revisited, showcasing holistic rectifier and antenna-based solutions which enable WPT and SWIPT to be implemented in real-world use-cases. Firstly, the challenge of efficiently rectifying low power levels using commercial Schottky diodes is addressed, in Section 2, through non-linear antenna-rectifier co-design. In Section 3, SWIPT based on shared-aperture antennas is described, showing a dual-band implementation. The scalability of co-designed rectennas is then demonstrated through a state-of-the-art rectenna array with an effective area exceeding its physical size, in Section 4. Finally, Section 5 highlights examples where mmWave wireless power can outperform its sub-6 GHz counterparts, and showcases the implementation of a wearable K-band rectenna using textile materials.

2 Antenna-Rectifier Co-Design: Non-Linear Optimization

The key challenge in long-range RF wireless power transfer (WPT) for low-power applications is converting µW inputs, efficiently, to DC. The Power Conversion Efficiency (PCE) at sub-0 dBm power levels is limited by the forward voltage drop across the rectifying diodes (or transistors) [3]. In addition, given the diodes' non-linearity, the rectifier's matching should be optimized for the target (low) RF power level. While source and load-pull contours have been widely used to optimize the performance of RF rectifiers for maximum RF to DC PCE, the key objective of the optimization process can vary the achieved efficiency [6]. To explain, the S_{11} of the rectifier, relative to a Z_0=50 Ω, is often observed in the source-pull optimization process. However, as the main parameter of interest in an RF rectifier is its DC output, at a given power level, a process of source and load pulling for maximizing the RF to DC PCE is proposed.

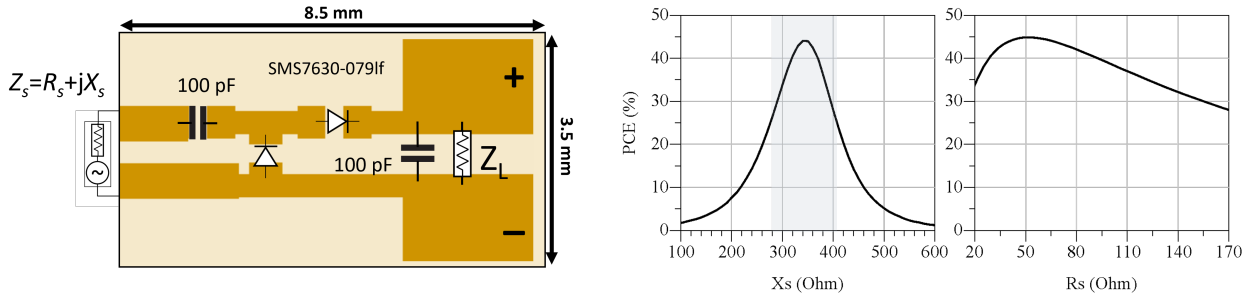

Figure 1: The non-linear/EM hybrid rectifier model used for harmonic balance large-signal optimization, at −20 dBm, and its simulated RF to DC PCE as a function of the imaginary (X_S) and real (R_S) input impedances [7].

The proposed method of maximising the rectifier's PCE relies on modelling the antenna as a complex-impedance source, which assumes the impedance matching will be done through the antenna as opposed to a standalone matching network. The DC load is then considered to be a static resistive load and both the source (complex) and load (resistive) impedances are iteratively swept to identify the optimum source and load impedances [7]. An example rectifier is shown in Figure 1, based on low-barrier silicon Schottky diodes (Skyworks SMS7630-079LF) in a voltage doubler configuration. The rectifier was simulated using Harmonic Balance (HB) technique in Keysight ADS, and was optimized for sub-1 GHz (868/915 MHz) applications.

Figure 1 shows the simulated PCE at −20 dBm which can approach 45%; the highest PCE achieved in prior works utilizing the same diode are under 35% [7]. This is due to the fact that the optimum impedance point shifts as the power level accepted by the diode increases, due to the junction's non-linearity. Therefore, the iterative optimization is a critical part of the rectifier matching process. While the extracted complex input impedance can be transformed to match a 50 Ω source, to maximise the compatibility with different antennas and arrays, a matching network implemented using discrete components such as lumped inductors incurs additional insertion losses which degrade the PCE [8]. On the other hand, designing an antenna to directly match the extracted impedance, e.g., Z=50+j330 Ω, can mitigate the additional insertion losses due to the very high radiation efficiency of a dipole implemented on a thin dielectric substrate such as polyimide and using copper as a conductor.

3 Antenna-Based Matching for SWIPT

In this section, the proposed approach of optimizing the rectifier and co-designing an energy harvesting antenna is demonstrated in a SWIPT application. In wireless communication literature, SWIPT is often addressed based on power-splitting or scheduling mechanisms, with multi-antenna solutions having a drawback of being more complex due to requiring multiple co-located antennas [9]. The proposed dual-band SWIPT systems is based on a shared-aperture antenna, using the lower frequency, around the 868 and 915 MHz license-free band, for WPT, and the 2.4 GHz band for communication. The system is evolved from a common geometry microstrip patch antenna, designed to radiate at 2.4 GHz. The patch, fed using a proximity-coupled microstrip line, has a second port added with an inductive loop feeding mechanism, enabling horizontally-polarized radiation from the second port along with a tunable inductive impedance [10, 11]. However, the radiation efficiency at the second port will be extremely low due to the lack of a radiating element. The ground plane of the patch is re-sized and dipole-like radiating arms are added to the patch; the dipole-like radiators are folded to miniaturize the antenna. Figure 2(a) shows the geometry of the novel dual-port microstrip antenna and its application in a SWIPT system.

Owing to the orthogonal feeding mechanism of the radiators, the antenna achieves high power isolation. Furthermore, as the rectifier's port is matched to a complex impedance, the mutual coupling between both ports is reduced further. Figure 2(b) shows the simulated (dashed) and measured (solid) S_{11} at the communication port, matched to 50 Ω in the 2.4 GHz band, and the mutual coupling (S_{21}) between both ports. In both the WPT and communication bands, the S_{21} is under −30 dB, which indicates that the far-field gain at both ports will not be compromised. Figure 2(c) shows the measured radiation patterns of the antenna at 2.4 GHz, where it can be seen that the presence of the rectifier does not affect the radiation on the body; the detailed co- and cross-polarized radiation properties are presented in [10].

To demonstrate a novel application of the antenna, it is implemented on a textile substrate, using shielding fabrics as conductive traces, for wearable SWIPT; wearable rectennas have been widely demonstrated using textile materials and are expected to be a key application of flexible and textile-integrated electronics [12, 13, 14, 6]. The broadside 2.4 GHz beam is particularly beneficial in communicating with an off-body device, and isolating the antenna from the human body enabling its radiation efficiency to be maintained. As for the sub-1 GHz broad-beam WPT application, it was previously shown that sub-1 GHz dipoles are capable of receiving

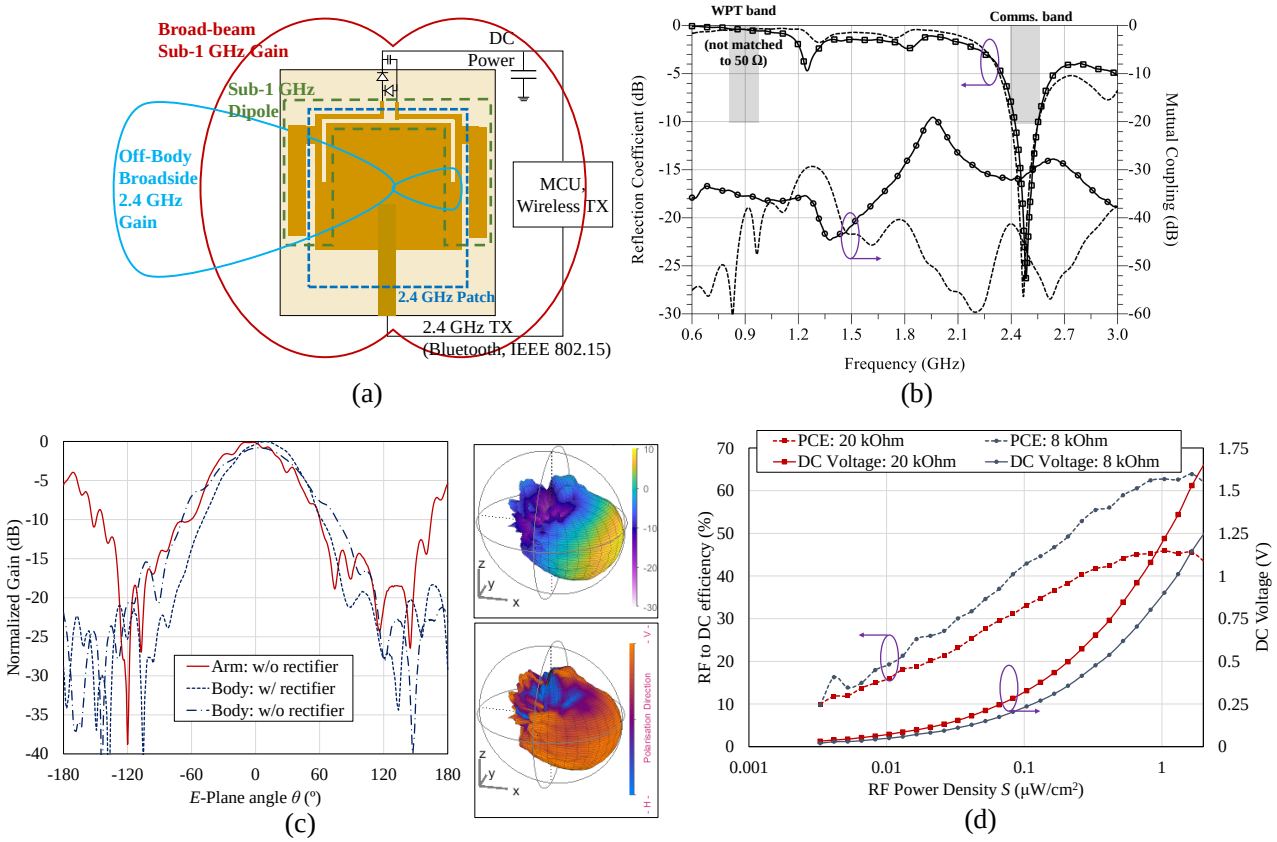

Figure 2: Antenna-enabled SWIPT using a shared quasi-microstrip radiating aperture: (a) a dual-band broadbeam/uni-directional antenna/rectenna operating in license-free bands (©IEEE 2021); (b) measured s-parameters of the antenna showing the high isolation between the power harvesting and communication ports; (c) measured radiation patterns of the antenna, at its 2.4 GHz communication port, over the E-plane in the presence and absence of the rectifier on-body, and the 3D directivity and polarization patterns on the body; (d) measured RF to DC PCE and DC voltage output for varying RF power densities at 830 MHz [10].

more power on the body than higher gain 2.4 GHz counterpart, due to their wider angular coverage and reduced body shadowing [15]. A total antenna efficiency of 63% was measured on a human body phantom at 2.4 GHz relative to a loss-less monopole over a large ground plane. The antenna's far-field patterns, in the main broadside beam, were similar (within 0.5 dB) in the presence and the absence of the rectifier.

The WPT performance of the dual-mode dual-band antenna/rectenna was evaluated wirelessly using a directional antenna, in the far-field, with a varying RF input to change the incident RF power density S. Following a frequency sweep where 820 MHz was found to be the frequency at which the rectenna achieved the maximum PCE, S was swept at 830 MHz; the DC output across two resistive loads was measured. Figure 2(d) shows the measured PCE and DC voltage, across a high-impedance (20 kΩ) and optimum (8 kΩ) load. The PCE was calculated relative to the received power using the simulated gain of the antenna; the communication port was terminated with a broadband 50 Ω resistor to emulate simultaneous information reception.

Due to the high isolation between the ports, observed in Figure 2(b), and the optimal rectifier matching, the proposed antenna achieved the highest radiation efficiency in its communication mode at 2.4 GHz, compared to previously reported wearable antennas based on similar materials [10]. Furthermore, the rectenna achieved the highest reported PCE of a flexible textile-based rectenna, [12, 13, 14, 6] , for a 1 μW/cm^2 incident power density. With such lossy dielectrics (tanδ=0.026) and conductors (Sheet resistance>0.02 Ω/square), eliminating the matching network and directly matching the rectifier using the antenna's impedance is crucial for achieving the high PCE shown in Figure 2(d).

4 Large-Area Arrays using Electrically-Small Antennas

While it was observed in Section 2 and 3 that a high RF to DC PCE can be achieved through the complex impedance tuning stage, the voltage output of individual rectennas is still limited for practical applications [16]. Rectenna arrays, also referred to as energy harvesting surfaces, have been widely proposed as a solution [17]. Nevertheless, their efficiency and sensitivity, to low RF inputs, has consistently been limited by their physical aperture. This is attributed to the large inter-element spacing, and choosing aperture-type harvesting elements.

Here, we show that using electrically-small rectennas elements, tightly-coupled to each other, an energy harvesting aperture larger than the array's physical aperture can be realized [18]. To explain, it is widely known that a dipole antenna, based on an infinitesimally-thin wire, has an effective receiving aperture that is significantly larger than its physical footprint [19]. This has previously motivated the use of overlapped antennas, stacked in the same area [20]. However, the individual rectenna elements did not have an optimized impedance to maximize the PCE, and the results were not scaled or characterized over different power levels.

The proposed array utilizes dipole elements with a tunable complex impedance, to enable the rectifiers to be presented with their optimum input impedance, extracted based on the process in Section 2. Figure 3(a) shows the implemented six-element array along with its associated DC power management stage, to enable the low voltage output to start conventional electronics running at >1.8 V. The antenna elements are based on the design first proposed in [21]. The array was evaluated wirelessly under varying RF power densities; the energy harvesting figure of merit was defined as

$$\text{FoM} = \frac{P_D C}{S A_{\text{physical}}} \tag{1}$$

where $P_D C$ is the array's DC output, S is the incident RF power density, and A is the array's physical area [18]. Eq. (1) combines both the antenna's size with the rectifier's efficiency and would lead to FoM>1 for a harvester with an effective area larger than its physical aperture A. This definition has been widely used to calculate the efficiency of finite energy harvesting surfaces [22, 23, 24].

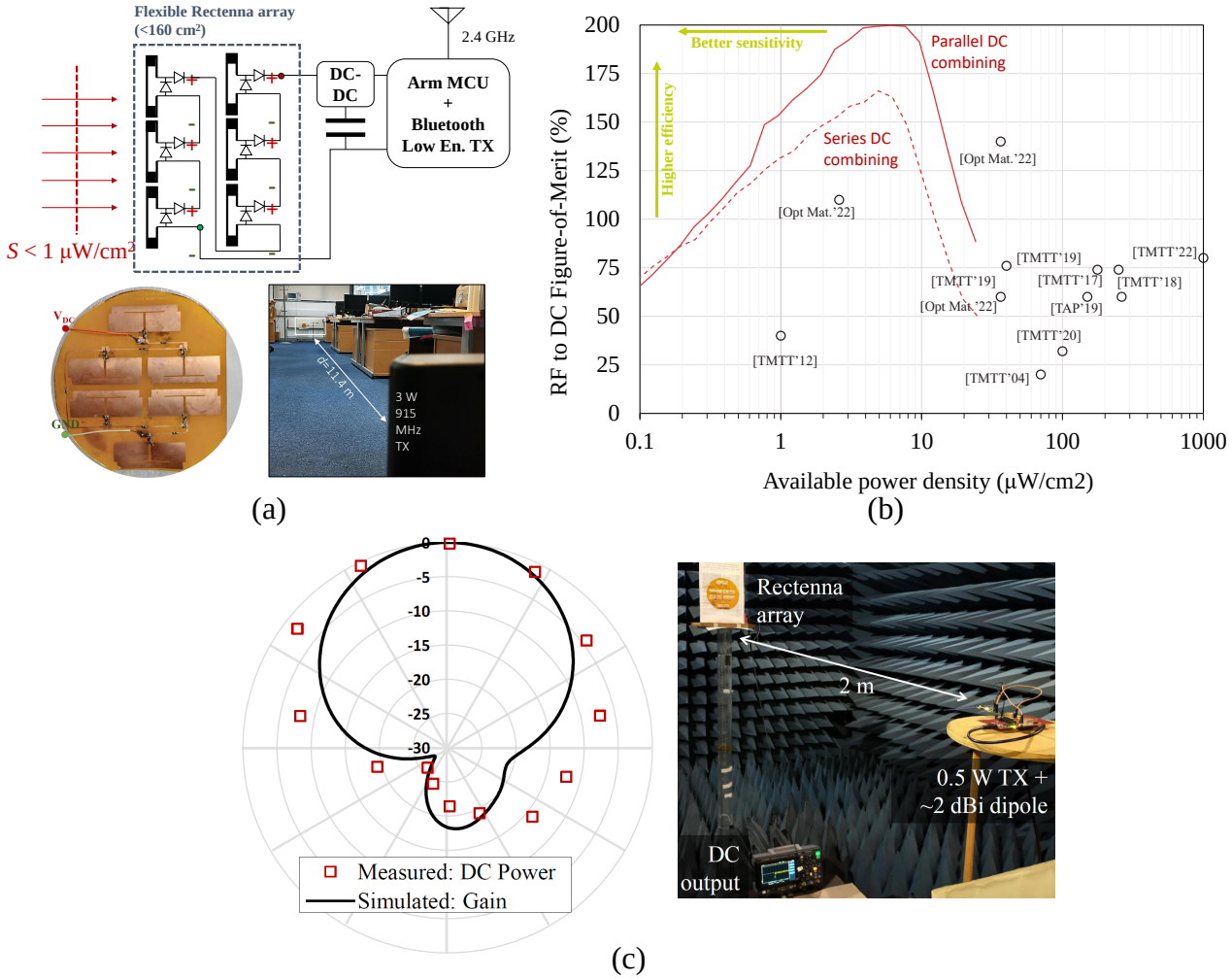

Figure 3: Scaled-up DC-combining rectenna array for low-power harvesting: (a) the array's system-level schematic, photograph, and indoor measurement setup; (b) measured RF to DC figure of merit, using (1), for varying power densities compared to prior energy harvesting surfaces, the detailed numerical comparison is in [18]; (c) the DC power harvesting patterns and simulated gain patterns of a reflector-backed broadside array and the anechoic chamber measurement setup [18].

Figure 3(b) shows the measured FoM, calculated using (1), of the proposed array and compares it to reported state-of-the-art large-scale RF energy harvesters; a detailed numerical comparison table can be found in [18]. From Figure 3(b), the advantage of using a large array based on tightly-coupled rectenna elements optimized for a high RF to DC efficiency can be seen. To explain, for an incident power density between 1 and 10 W/cm^2,

the proposed surface maintains a collection area that is over 150% its physical footprint, which is attributed to the use of tightly-coupled electrically-small rectenna elements.

The high sensitivity of the rectennas and the combined output translates to a very high voltage sensitivity; the series DC voltage combining leads to a 1 V DC output across a 40 kΩ load at 10 m from a 3 W license-free 915 MHz source. With the aid of a commercially-available DC-DC boost converter (Texas Instruments BQ25504), a Bluetooth Low Energy (BLE) wireless sensor node was experimentally demonstrated cold-starting from a 0.22 μW/cm^2 incident power density, achieving an unprecedented sensitivity using a low-cost, single-layered conformable array [18].

In its free-standing low-profile (<1 mm-thick) format, the array maintains an omnidirectional DC power harvesting pattern. However, in applications where the direction of incidence of the RF power is known, it is desirable to maintain a unidirectional harvesting pattern. To realize the broadside harvesting pattern, reflector-backing is proposed. Figure 3(c) shows, for the first time, the measured DC voltage output of the proposed surface for different angles of incidence with an electrical reflector placed at a 0.1 λ separation from the array. The array's single-element radiation pattern was simulated in full-wave electromagnetic simulation (CST Microwave Studio) and is shown alongside the measured DC patterns in Figure 3(c); the array's DC patterns were characterized at 2 m from the source in an anechoic chamber, as shown in the photograph in Figure 3(a).

The reflector backing results in a 4 dB increase in the received DC power in the broadside direction. The reflector-backed array maintains over 15 dB front-to-back ratio. The thickness of the overall prototype can be further reduced by utilizing an artificial magnetic conductor (AMC).

5 Wireless Power at mmWave Frequencies

The presented WPT and SWIPT solutions in the previous sections were limited to sub-6 GHz frequencies. However, network-level calculations have previously shown that a higher end-to-end efficiency can be achieved at mmWave frequencies [25]. Considering the free space path loss formula

$$P_{RX} = P_{TX} G_{TX} G_{RX} (\frac{c}{4\pi f d})^2, \tag{2}$$

where f is the frequency, d is the transmitter-receiver distance, it can be seen that operating a wireless power link at a higher frequency leads to an exponentially higher path loss. However, both the transmitting and receiving gains $G_{TX/RX}$ are also frequency-dependent for a the same aperture size. Re-writing the aperture efficiency formula, the gain of an electrically-large aperture is a function of the antenna's physical size and its aperture efficiency, and is given by

$$G = \frac{4\pi\eta f^2}{c^2} A_{\text{phys}}. \tag{3}$$

G is the antenna's gain, f is the frequency, c is the speed of light, η is the aperture efficiency, and A_{phys} is the antenna's physical area [19]. Substituting (3) in (2), for both the transmitting and receiving antennas, the received-to-transmitted power is given by

$$\frac{P_{\text{RX}}}{P_{\text{TX}}} = \frac{1}{c^2 d^2} A_{\text{TX}} A_{\text{RX}} \eta_{\text{TX}} \eta_{\text{RX}} f^2, \tag{4}$$

where TX and RX correspond to the transmitter and receiver's size and aperture efficiency [26]. From (4), it can be seen that, assuming a constant aperture efficiency and fixed physical areas, a higher end-to-end WPT efficiency can be achieved by operating at higher frequencies.

The performance of practical WPT link, illustrating (4), for a 100 m distance with 10×10 cm^2 transmitting and receiving antenna is shown in Figure 4(a). It can be seen that assuming a uniform and ideal aperture, a higher WPT efficiency can be achieved by operating at higher frequencies. While this calculation does not include atmospheric attenuation, the attenuation is less than 1 dB/km under 50 GHz [27].

While the RF link efficiency shows potential performance gains at mmWave bands, assuming a high aperture efficiency can be achieved, the mmWave to DC PCE still represents a significant bottle-neck [26]. In implementing a mmWave rectenna, targeting low-cost wearable application, a 50 Ω-matched antenna and a rectifier with a standalone matching network are chosen. This simplifies the characterization of both the antenna and the rectifier separately using standard 50 Ω instruments. Moreover, the datasheet diode models can underestimate the total capacitance and junction resistance for the devices [29, 30], implying that the non-linear co-design process introduced in Section 2 could lead to inaccurate source and load impedance values.

The rectifier was designed based on a Macom GaAs MA4E1319 series-pair flip-chip diodes, matched using a tapered inductive microstrip line to achieve a broadband match which covers the 5G 26 and 28 GHz frequency bands. While this limited the S_{11} to a maximum of −3 dB, it maximized the half-power bandwidth of the rectenna. As for the antenna, the broadband antipodal Vivaldi-inspired monopole achieves an $S_{11} < -10$ dB bandwidth from 24 to 40 GHz, with a measured 67% total efficiency at 24 GHz, inclusive of the microstrip

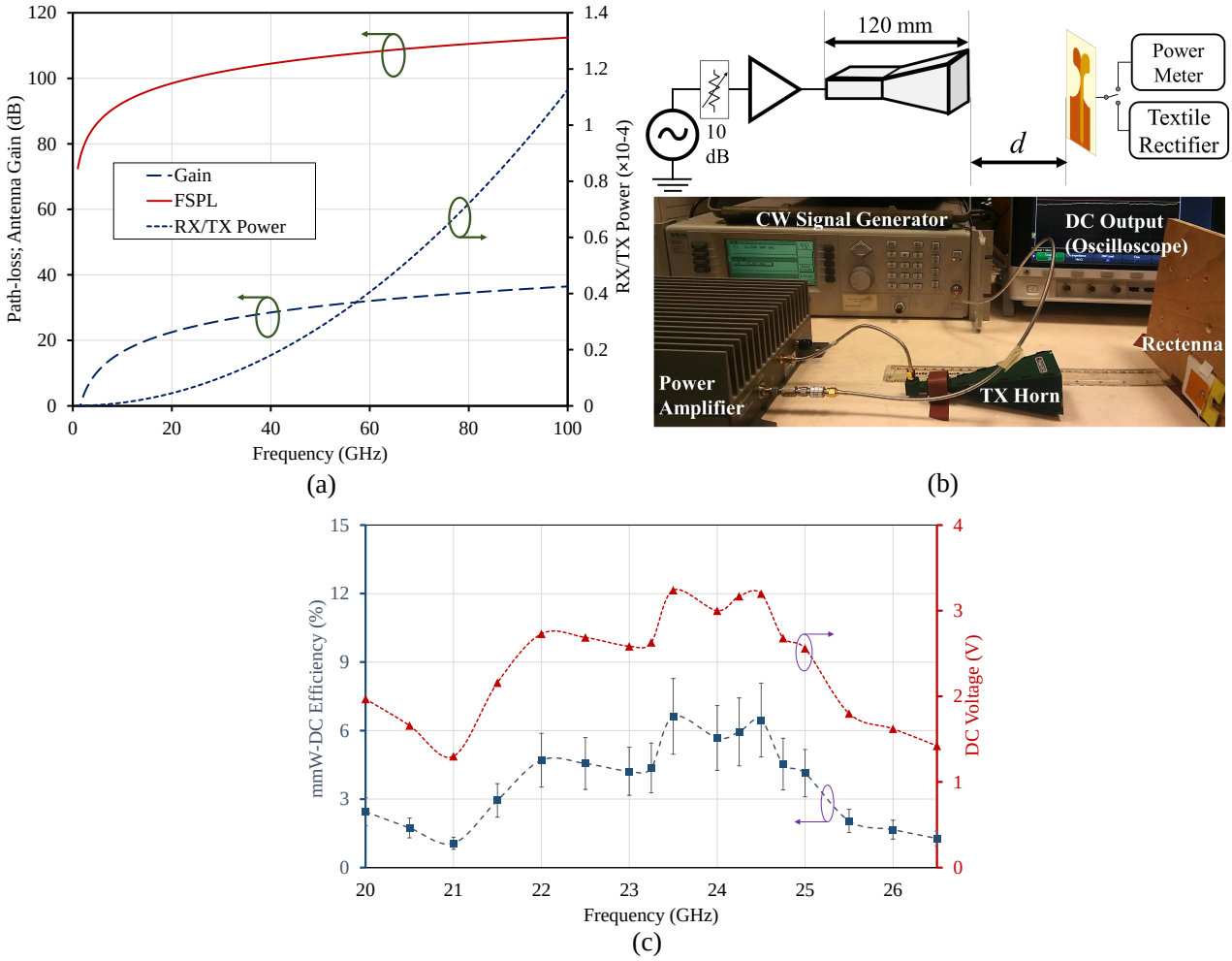

Figure 4: WPT at mmWave frequencies: (a) analytically calculated received/transmitted power ratio over frequency assuming fixed transmitting and receiving antenna area and aperture efficiency, as well as beam alignment [26]; (b) measurement setup of a K-band rectenna based on a Vivaldi-inspired wearable antenna and GaAs diodes; (c) measured mmWave to DC PCE and DC voltage output, across a high-impedance 10 kΩ load, for an estimated 10 dBm input [28].

feed losses connecting the rectifier. The achieved efficiency and bandwidth are higher than previously reported mmWave antennas implemented on textile substrates [28, 31], which are characterised by a tanδ >0.02.

The mmWave rectenna was characterized wirelessly using a 1 W saturated-output amplifier and a 20 dBi horn. As a far-field measurement was not possible due to the low power output of the amplifier, the incident power level was estimated using a power meter connected to a connectorized version of the same antenna. The measured received mmWave power was used calculate the PCE and estimate the rectenna's sensitivity. Figure 4(c) shows the measured DC voltage output and PCE for a 10 dBm input across the K-band. The measurements were limited to 26.5 GHz due to the amplifier's limited bandwidth, but it can be seen from the DC output curve that the rectenna could be used above 26.5 GHz. While a 10 dBm input is unlikely to be achieved at a range exceeding 10 cm from a 1 W source, the FCC's EIRP in teh 5G 28 GHz bands is 75 dBm. With a 75 dBm EIRP and a 10 m source-rectenna distance, 2 dBm can be received, which enables the rectenna to generate a sufficient DC output [28].

The implementation of the textile-based rectenna combined multiple fabrication steps to maintain flexibility and mechanical reliability. The rectifier was fabricated using photolithography on a copper-clad polyimide substrate, which is then adhered to the wearable textile substrate for monolithic integration with the antenna. Figure 5(a) shows the wafer used to prototype multiple antenna designs, and the rectenna's traces before being assembled with the components mounted, in Figure 5(b). For such a fragile yet mechanically flexible circuit, encapsulation of the most sensitive component, the diode chip, is required. This is achieved using UV curable glob-top epoxy, with the bare die and encapsulated diodes visible in Figure 5(c) and (d), respectively. While no mechanical stressing tests were carried out on this prototype, previously reported textile-based flip-chip ICs packaged using the same technique were demonstrated working reliably for up to 10,000 bending cycles [32]. Further improvements in the mechanical reliability can be achieved by laminating the entire structure; this was previously validated in a 50 GHz microstrip-integrated DC-blocking capacitor on a textile substrate [33].

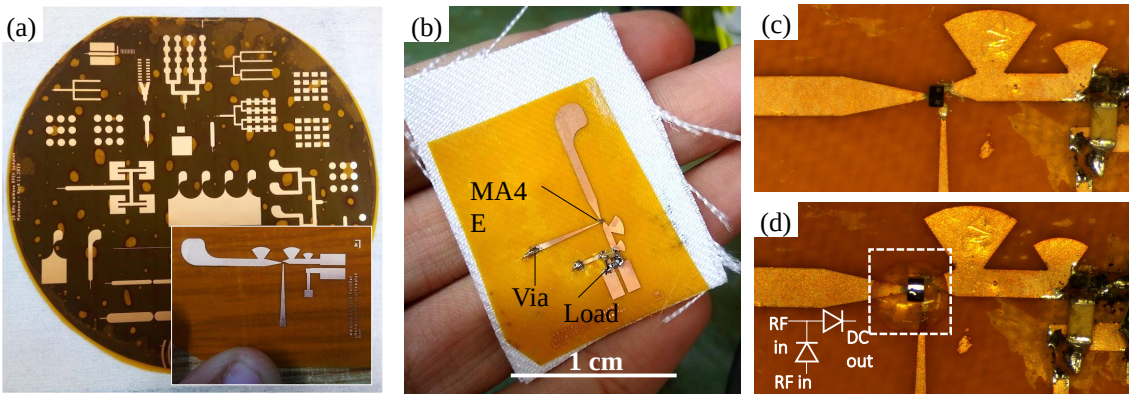

Figure 5: The fabricated textile-based mmWave rectenna prototypes: (a) single-layer photolithography of the polyimide-copper laminates; (b) the assembled rectenna with a flexible through-fabric via; (c) the bonded GaAs diodes chip on the copper traces; (d) glob-top-encapsulated diodes for mechanical reliability [28].

6 Conclusions

This paper presented an overview of designing rectennas for low-power WPT and SWIPT applications. A standard approach of tuning the source and load impedances of a rectifier circuit, with the objective of maximising the DC output was outlines, and demonstrated for practical Schottky diodes. The scalability of the rectifier design methodology was applied in a SWIPT rectenna and a large-area flexible rectenna array, demonstrating state-of-the-art RF to DC PCE in both applications. Finally, the opportunities and challenges of implementing WPT systems in the mmWave spectrum were highlighted in wearable application integrating commercially-available devices with flexible textile-based passives.

To allow the developed rectennas to be utilized in real-world applications, efficient DC to RF power transmitters need to be realized. In addition, an effective narrow-band and power-optimized modulation scheme, to allow power and data to be simultaneously transmitted, is required. At a device-level, WPT-specific diodes are required for both low and high-power applications, where the majority of existing rectenna research is based on commercial devices intended for detectors and mixers. Monolithic integration of more complex and potentially tunable rectifier circuits based on optimally-sized devices could enable high sensitivities and efficiencies to be achieved, particularly at mmWave frequencies.

Acknowledgment

The author would like to thank S. Beeby, A. Weddell, and G. Hilton for supporting the work and providing access to experimental facilities. The work of M. Wagih is supported by the UK Royal Academy of Engineering (RAEng) and the Office of the Chief Science Adviser for National Security under the UK Intelligence Community Post-Doctoral Research Fellowship programme. This work was jointly supported by the UK Engineering and Physical Sciences Research Council (EPSRC) under Grant EP/P010164/1 and the European Commission through the project EnABLES, funded under H2020-EU.1.4.1.2 grant number: 730957.

References

[1] W. Brown, "The history of power transmission by radio waves," *IEEE Transactions on Microwave Theory and Techniques*, vol. 32, no. 9, pp. 1230–1242, 1984.

[2] C. T. Rodenbeck, P. I. Jaffe, B. H. Strassner II, P. E. Hausgen, J. O. McSpadden, H. Kazemi, N. Shinohara, B. B. Tierney, C. B. DePuma, and A. P. Self, "Microwave and millimeter wave power beaming," *IEEE Journal of Microwaves*, vol. 1, no. 1, pp. 229–259, 2021.

[3] C. R. Valenta and G. D. Durgin, "Harvesting Wireless Power: Survey of Energy-Harvester Conversion Efficiency in Far-Field, Wireless Power Transfer Systems," *IEEE Microw. Mag.*, vol. 15, 4, pp. 108–120, 2014.

[4] X. Gu, L. Grauwin, D. Dousset, S. Hemour, and K. Wu, "Dynamic Ambient RF Energy Density Measurements of Montreal for Battery-Free IoT Sensor Network Planning," *IEEE Internet of Things Journal*, pp. 1–1, 2021.

[5] X. Lu, P. Wang, D. Niyato, D. I. Kim, and Z. Han, "Wireless Networks With RF Energy Harvesting: A Contemporary Survey," *IEEE Communications Surveys & Tutorials*, vol. 17, 2, pp. 757 – 789, 2015.

[6] J. A. Estrada, E. Kwiatkowski, A. López-Yela, M. Borgoñós-García, D. Segovia-Vargas, T. Barton, and Z. Popović, "An RF-Harvesting Tightly-Coupled Rectenna Array Tee-Shirt with Greater than Octave Bandwidth," *IEEE Trans. Microw. Theory Techniq.*, vol. 68 no. 9, pp. 3908 – 3919, 2020.

[7] M. Wagih, A. S. Weddell, and S. Beeby, "High-Efficiency Sub-1 GHz Flexible Compact Rectenna based on Parametric Antenna-Rectifier Co-Design," in *2020 IEEE/MTT-S International Microwave Symposium (IMS)*, 2020.

[8] ——, "Omnidirectional Dual-Polarized Low-Profile Textile Rectenna with over 50% Efficiency for Sub-μW/cm^2 Wearable Power Harvesting," *IEEE Transactions on Antennas and Propagation*, vol. 69, no. 5, pp. 2522–2536, 2021.

[9] T. D. P. Perera, D. N. K. Jayakody, S. K. Sharma, S. Chatzinotas, and J. Li, "Simultaneous Wireless Information and Power Transfer (SWIPT): Recent Advances and Future Challenges," *IEEE Communication Surveys and Tutorials*, vol. 20, 1, pp. 264 – 302, 2018.

[10] M. Wagih, G. S. Hilton, A. S. Weddell, and S. Beeby, "Dual-Band Dual-Mode Textile Antenna/Rectenna for Simultaneous Wireless Information and Power Transfer (SWIPT)," *IEEE Transactions on Antennas and Propagation*, vol. 69, no. 10, pp. 6322–6332, 2021.

[11] ——, "Dual-Polarized Wearable Antenna/Rectenna for Full-Duplex and MIMO Simultaneous Wireless Information and Power Transfer (SWIPT)," *IEEE Open Journal of Antennas and Propagation*, vol. 2, pp. 844–857, 2021.

[12] S.-E. Adami, P. Proynov, G. S. Hilton, G. Yang, C. Zhang, D. Zhu, Y. Li, S. P. Beeby, I. J. Craddock, and B. H. Stark, "A Flexible 2.45-GHz Power Harvesting Wristband With Net System Output From -24.3 dBm of RF Power," *IEEE Trans. Microw. Theory Techn.*, vol. 66 no. 1, pp. 380–395, 2018.

[13] G. Monti, L. Corchia, and L. Tarricone, "UHF Wearable Rectenna on Textile Materials," *IEEE Trans. Antennas. Propag.*, vol. 61, 7, pp. 3869 – 3873, 2013.

[14] D. Vital, S. Bhardwaj, and J. L. Volakis, "Textile Based Large Area RF-Power Harvesting System for Wearable Applications," *IEEE Trans. Antennas Propag.*, vol. 68, no. 3, pp. 2323 – 2331, 2019.

[15] M. Wagih, O. Cetinkaya, B. Zaghari, A. S. Weddell, and S. Beeby, "Real-World Performance of Sub-1 GHz and 2.4 GHz Textile Antennas for RF-Powered Body Area Networks," *IEEE Access*, vol. 8, pp. 133 746 – 133 756, 2020.

[16] A. Shrivastava, N. E. Roberts, O. U. Khan, D. D. Wentzloff, and B. H. Calhoun, "A 10 mV-Input Boost Converter With Inductor Peak Current Control and Zero Detection for Thermoelectric and Solar Energy Harvesting With 220 mV Cold-Start and -14.5 dBm, 915 MHz RF Kick-Start," *IEEE Journal of Solid-State Circuits*, vol. 50, 8, pp. 1820 –1832, 2015.

[17] E. Kwiatkowski, J. A. Estrada, A. López-Yela, and Z. Popović, "Broadband RF Energy-Harvesting Arrays," *Proceedings of the IEEE*, vol. 110, no. 1, pp. 74–88, 2022.

[18] M. Wagih and S. Beeby, "Thin flexible rf energy harvesting rectenna surface with a large effective aperture for sub w/cm2 powering of wireless sensor nodes," *IEEE Transactions on Microwave Theory and Techniques*, vol. 70, no. 9, pp. 4328–4338, 2022.

[19] C. A. Balanis, "Antenna Theory: Analysis and Design. Third Edition," *Wiley Interscience*, pp. 84 – 85, 2005.

[20] M. Mi, M. Mickle, C. Capelli, and H. Swift, "Rf energy harvesting with multiple antennas in the same space," *IEEE Antennas and Propagation Magazine*, vol. 47, no. 5, pp. 100–106, 2005.

[21] M. Wagih, A. S. Weddell, and S. Beeby, "Meshed High-Impedance Matching Network-Free Rectenna Optimized for Additive Manufacturing," *IEEE Open Journal of Antennas and Propagation*, vol. 1, pp. 615 – 626, 2020.

[22] F. Erkmen, T. S. Almoneef, and O. M. Ramahi, "Scalable electromagnetic energy harvesting using frequency-selective surfaces," *IEEE Transactions on Microwave Theory and Techniques*, vol. 66, no. 5, pp. 2433–2441, 2018.

[23] T. S. Almoneef, F. Erkmen, M. A. Alotaibi, and O. M. Ramahi, "A New Approach to Microwave Rectennas Using Tightly Coupled Antennas," *IEEE Trans. Antennas Propag.*, vol. 66, 4, pp. 1714 – 1724, 2018.

[24] L. Li, X. Zhang, C. Song, W. Zhang, T. Jia, and Y. Huang, "Compact Dual-Band, Wide-Angle, Polarization-Angle-Independent Rectifying Metasurface for Ambient Energy Harvesting and Wireless Power Transfer," *IEEE Trans. Microw. Theory Techn.*, vol. Early Access, DOI: 10.1109/TMTT.2020.3040962, 2020.

[25] T. A. Khan, A. Alkhateeb, and R. W. Heath, "Millimeter Wave Energy Harvesting," *IEEE Trans. Wireless Communications*, vol. 15, 9, pp. 6048 – 6062, 2016.

[26] M. Wagih, A. S. Weddell, and S. Beeby, "Millimeter-Wave Power Harvesting: A Review," *IEEE Open Journal of Antennas and Propagation*, vol. 1, pp. 560 – 578, 2020.

[27] I. A. Hemadeh, K. Satyanarayana, M. El-Hajjar, and L. Hanzo, "Millimeter-Wave Communications: Physical Channel Models, Design Considerations, Antenna Constructions, and Link-Budget," *IEEE Communications Surveys & Tutorials*, vol. 20, 2, pp. 870 – 913, 2017.

[28] M. Wagih, G. S. Hilton, A. S. Weddell, and S. Beeby, "Broadband Millimetre-Wave Textile-based Flexible Rectenna for Wearable Energy Harvesting ," *IEEE Trans. Microw Theory Techn*, vol. 68 no. 11, pp. 4960 – 4972, 2020.

[29] J. Bito, V. Palazzi, J. Hester, R. Bahr, F. Alimenti, P. Mezzanotte, L. Roselli, and M. M. Tentzeris, "Millimeter-wave ink-jet printed RF energy harvester for next generation flexible electronics," in *2017 IEEE Wireless Power Transfer Conference (WPTC)*, 2017.

[30] S. Hemour, C. H. P. Lorenz, and K. Wu, "Small-footprint wideband 94 GHz rectifier for swarm microrobotics," in *2015 IEEE MTT-S International Microwave Symposium*, 2015.

[31] N. Chahat, M. Zhadobov, S. A. Muhammad, L. L. Coq, and R. Sauleau, "60-GHz Textile Antenna Array for Body-Centric Communications," *IEEE Trans. Antennas Propag.*, vol. 61 no. 4, pp. 1816 – 1824, 2013.

[32] A. Komolafe, R. Torah, Y. Wei, H. Nunes-matos, M. Li, D. Hardy, T. Dias, M. Tudor, and S. Beeby, "Integrating flexible filament circuits for e-textile applications," *Advanced Materials Technologies*, vol. 4, no. 7, 2019.

[33] M. Wagih, A. Komolafe, and N. Hillier, "Screen-printable flexible textile-based ultra-broadband millimeter-wave dc-blocking transmission lines based on microstrip-embedded printed capacitors," *IEEE Journal of Microwaves*, vol. 2, no. 1, pp. 162–173, 2022.